

In vivo optogenetics reveals homeostatic control of cochlear sensitivity by supporting cells

Victoria Lukashkina

University of Brighton

Snezana Levic

University of Brighton

Patricio Simões

University of Brighton

Zhenhang Xu

Creighton University School of Medicine

Joseph DiGuseppi

Creighton University School of Medicine

Jian Zuo

Creighton University

Andrei Lukashkin

University of Brighton <https://orcid.org/0000-0003-4577-8716>

Ian Russell (✉ I.Russell@brighton.ac.uk)

University of Brighton <https://orcid.org/0000-0002-4915-2772>

Article

Keywords: In vivo, optogenetics, homeostatic control, cochlear sensitivity, supporting cells

Posted Date: October 20th, 2020

DOI: <https://doi.org/10.21203/rs.3.rs-92461/v1>

License:   This work is licensed under a Creative Commons Attribution 4.0 International License.

[Read Full License](#)

In vivo optogenetics reveals homeostatic control of cochlear sensitivity by supporting cells

Authors: Victoria A. Lukashkina¹, Snezana Levic^{1,3}, Patricio Simões^{1†}, Zhenhang Xu², Joseph A. DiGiuseppi², Jian Zuo^{2*}, Andrei N. Lukashin^{1*}, Ian J. Russell^{1*}

Affiliations:

¹Sensory Neuroscience Research Group, School of Pharmacy and Biomolecular Sciences, University of Brighton, Huxley Building, Brighton, BN2 4GJ, UK

²Department of Biomedical Sciences, Creighton University School of Medicine, 2500 California Plaza, Omaha, NE 68178, USA

³Brighton and Sussex Medical School, University of Sussex, Brighton BN1 9PX, UK.

†Current address: Sussex Neuroscience, School of Life Sciences, University of Sussex, Brighton BN1 9QG, UK

*Correspondence to: A.Lukashkin@brighton.ac.uk, I.Russell@brighton.ac.uk, JianZuo@creighton.edu

ABSTRACT:

We used optogenetics to investigate the control of auditory sensitivity by cochlear supporting cells that scaffold outer hair cells, which transduce and amplify cochlear responses to sound.

In vivo and *in vitro* measurements of sound-induced cochlear mechanical and electrical responses were made from mice that conditionally expressed nonselective cationic channelrhodopsins in Deiters' and outer pillar supporting cells in the organ of Corti. We demonstrated that cochlear light-stimulation and subsequent activation of channelrhodopsins depolarized the supporting cells, changed their extracellular electrical environment, and sensitized insensitive and desensitized sensitive cochlear responses to sound. We concluded that outer hair cells, Deiters' cells and outer pillar cells interact through feedback which regulates their immediate ionic and electrical environment and controls energy flow in the mammalian cochlea to optimize its performance over its entire dynamic range. Activation of the supporting cell channelrhodopsins shunts this feedback system and restores cochlear sensitivity to a set level.

32

33 INTRODUCTION

34 A striking feature of the mammalian sensory auditory epithelium, the organ of Corti (OC) of
35 the cochlea, is the cellular architecture and arrangement of the so-called supporting cells that
36 provide a structural scaffold for the sensory hair cells ¹. However, to date there have been no
37 direct *in vivo* evidence to show how supporting cells interact with hair cells to provide the
38 cochlea's sensitive, sharply tuned, responses to sound stimulation. The OC (Fig. 1a) is
39 attached to the extracellular matrix of the basilar membrane (BM), which spirals in graded
40 stiffness and frequency selectivity from the low-frequency apex to the high-frequency base of
41 the coiled cochlea, thereby spatially separating individual frequency components of complex
42 sounds into different locations on the BM according to the so-called characteristic frequency
43 (CF) of their location ². Of the two types of sensory cells located in the OC, the electromotile
44 outer hair cells (OHCs) ³⁻⁵ sense sound evoked BM vibrations through displacements of the
45 hair bundles, which alter the gating probability of mechano-electrical transduction (MET)
46 channels located near the tips of the stereocilia that comprise the hair bundles ⁶. Flow of
47 predominantly K⁺ current through the MET conductance, which is modulated during BM
48 sound-induced vibration ⁶, is driven by the batteries of the endocochlear potential (EP) and
49 OHC resting potential in series ⁷. The OHC MET currents generate receptor potentials that
50 produce transmembrane voltage differences which control ultrafast OHC electromotility that
51 power-amplifies and sharpens cochlear mechanical responses locally to frequencies close to
52 the CF ^{2,8}. OHC electromotility, and resultant cochlear amplification, is mediated by a protein
53 prestin, which is abundantly present in the OHC lateral membrane and changes its
54 conformation in response to OHC transmembrane voltage changes ⁸. The OHCs operate
55 within a structural scaffold of supporting cells, the outer pillar cells (OPCs) and Deiters' cells
56 (DCs), which encompass fluid-filled spaces of Nuel (SN) that envelope the lateral

57 membranes of the OHCs (Fig. 1a). The supporting cells, especially the DCs, are crucially
58 located to play instrumental roles in the passive and active transmission of forces from OHCs
59 to the structures of the cochlear partition and to control OHC axial loading^{9,10}. The apical
60 poles of the motile DCs^{11,12}, which also contribute to the OC electrical conductance^{13,14},
61 support the OHCs and transmit their forces to the cochlear partition. The long, stiff,
62 phalangeal processes of the DCs mechanically link the basal and apical poles of the OHCs,
63 forming a perfect feedback system for controlling the mechano-electrical energy flow within
64 the OC and hence cochlear sensitivity (^{15,16}, Fig. 1a). Thus, OHCs are enclosed in a potential
65 control system that could regulate their sensitivity through changes to their mechanical,
66 electrical, and ionic environment.

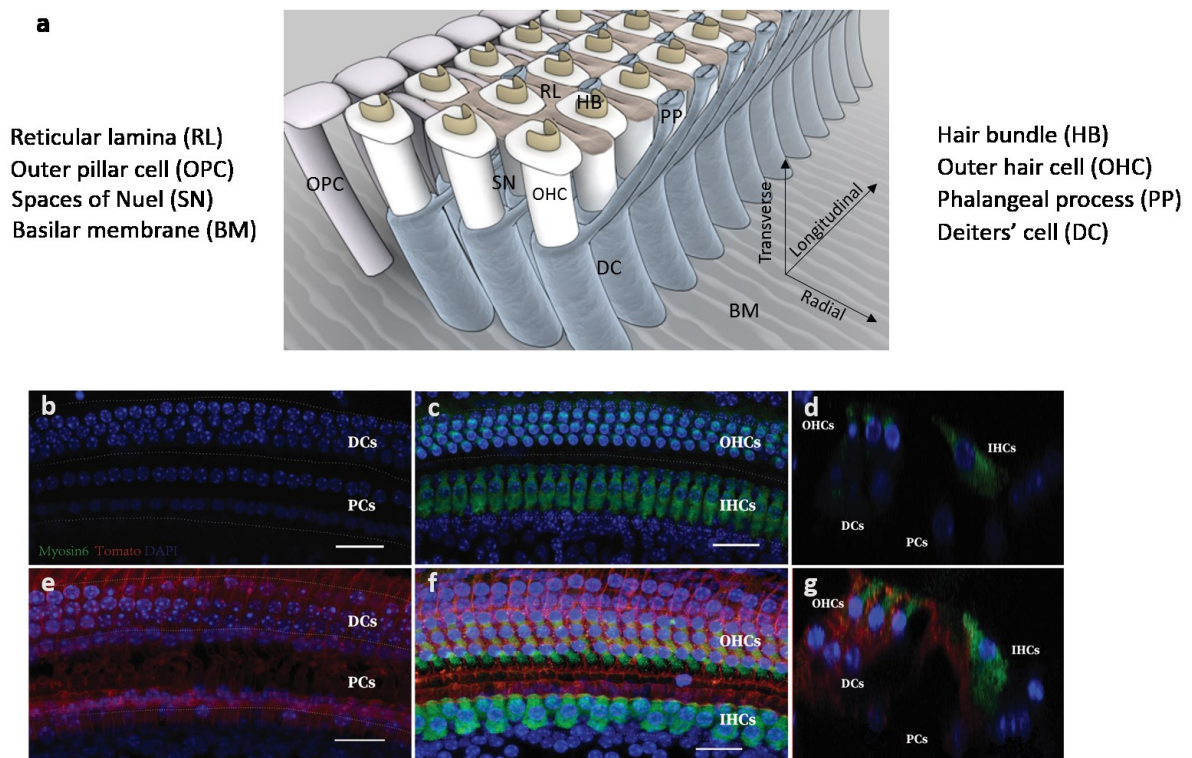
67 To test this hypothesis *in vivo*, we have exploited optogenetics and used mice with
68 conditional expression of COP-tdTomato channelrodopsin (COP) specifically in the DCs and
69 OPCs (Supplemental Methods and Fig. 1b-g). This approach provided the opportunity to
70 examine the involvement of DCs and OPCs in controlling the sensitivity of the cochlea and
71 revealed a novel homeostatic system of cochlear sensitivity regulation.

72 **RESULTS**

73 **Specific inducible expression of COP in cochlear supporting cells**

74 To induce COP expression specifically in mature DCs and PCs in the organ of Corti of the
75 cochlea, we used a previously characterized Fgfr3-iCreER^{T2} mouse line that displays ~100%
76 inducible Cre activity in cochlear DCs and PCs when tamoxifen was injected at juvenile and
77 adult ages^{17,18}. When induced at postnatal days 12 and 13 (P12/13) or P21, Fgfr3-
78 iCreERT2+; COP-tdTomato+ experimental mice showed robust expression of COP-
79 tdTomato fusion protein specifically in both DCs and PCs within the organ of Corti at P28,
80 whereas no COP-tdTomato was detected in DCs/PCs in Fgfr3-iCreERT2-; COP-tdTomato+

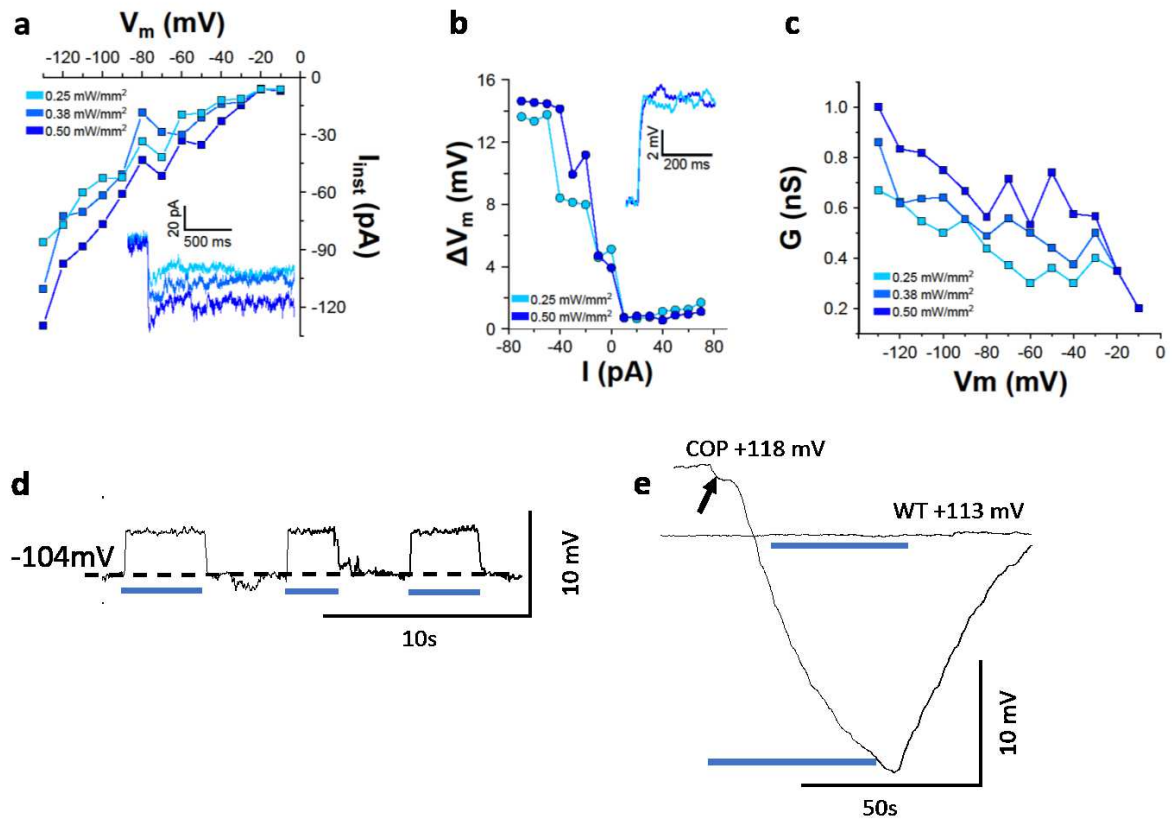
81 control mice at P28 (Fig. 1b-g; see Methods). No expression of COP-tdTomato fusion protein
 82 was detected in stria vascularis or any other cochlear structures of *Fgfr3-iCreERT2+*; COP-
 83 tdTomato⁺ experimental mice when induced at P12/13 and analyzed at P21/22. These results
 84 on COP specific expression in DCs and PCs in the cochlea are consistent with previous
 85 studies¹⁷⁻¹⁹.
 86



87
 88 **Figure 1. Schematic of the organ of Corti and expression of COP-tdTomato ChR in its supporting cells. (a)**
 89 Schematic of the radially distal region of the organ of Corti. **(b-g)** ChR expression in the DCs and inner and outer
 90 pillar cells (PCs). *Fgfr3-iCreERT2+*; COP-tdTomato mice were induced with tamoxifen (TMX) at P12/13 and
 91 analyzed at postnatal-day 28. **(b-d)** *Fgfr3-iCreERT2+*; COP-tdTomato⁺ control mice. **(e-g)** *Fgfr3-iCreERT2+*; COP-
 92 tdTomato⁺ experimental mice. **(b,c,e,f)** wholemount cochlear basal turns. **(b,e)** supporting cell layers. **(c,f)**
 93 projections of supporting cell and hair cell layers. **(d,g)** optical cross-sections in **(b,c)** and **(e,f)** respectively. IHCs:
 94 inner hair cells. Green: Myo6; blue: DAPI; red: autofluorescence of tdTomato. Scale bar = 20um.

95 **Cochlear illumination depolarizes COP mouse DC membrane potentials and reduces**
 96 **the endocochlear potential.**

97 COP is a light-sensitive cation selective channel^{20,21}. When activated by light, COP-
98 expressing DCs are depolarized (Fig. 2a,b) with increased conductance (Fig. 2c), which was
99 not observed in wild-type littermates in whole cell patch recordings from *ex vivo* flat-
100 mounted preparations of the OC. Depolarization, similar in magnitude to that recorded from
101 *ex vivo* COP expressing DCs, was recorded from presumed COP-expressing DCs (resting
102 potentials; -108.5 ± 8.7 mV, n = 25 DCs in 14 cochleae) when activated by illumination of
103 the BM and recorded with an intracellular micropipette *in vivo* (Fig. 2d,f). When advanced
104 (see Supplemental Methods) through the DCs, the micropipette encountered the positive
105 ($+114.3 \pm 3.7$ mV, n=11 mice) endocochlear potential (EP) of the scala media (Fig. 2e), one
106 of the batteries in series that drives receptor current through the gated OHC MET
107 conductance. At BM illumination onset, the EP was reduced by ~ 1 mV, which lasted without
108 decline for 1 – 3s followed by a steady decline in EP throughout the duration of the
109 illumination, falling by $23 \text{ mV} \pm 4 \text{ mV}$ in 40 s, n= 6. EP fully recovered to pre-illumination
110 levels when measured 3 to 5 minutes after BM illumination. Light-activated changes in EP
111 described above were not encountered in littermates that did not express COP in the DCs and
112 OPCs (Fig. 2e, WT trace). Altogether, these findings indicate that the DCs and OPCs are
113 essential components of the cochlear electrical network^{13,14} and their potential and
114 conductance changes can control the EP.



115

116 **Figure 2. Cochlear illumination depolarizes COP mouse DC membrane potentials and reduces the**

117 **endocochlear potential. (a) *Ex vivo* whole-cell patch recordings of current-voltage (I-V) plot: peak current**

118 **amplitudes of a DC elicited in response to laser illumination at different power densities, as functions of membrane**

119 **potential. Inset: Inward current traces at different laser power densities (-90 mV holding potential). (b) *Ex vivo***

120 **light-induced potential-current (ΔV -I) relationship of a DC: membrane potential changes (ΔV) during laser**

121 **illumination as functions of injected currents. Light-induced depolarizations were elicited during negative current**

122 **injection. Inset: whole-cell current-clamp recording (resting membrane potential = -50 mV) of light elicited**

123 **depolarization with different laser power densities. (c) Conductance G (nS) as a function of membrane potential**

124 **V (mV) at 3 different laser power densities using data in (a) at -130 mV holding potential. Increasing laser power**

125 **increased the DC membrane conductance (0.67, 0.86 and 1 nS respectively). (d) *In vivo* intracellular recordings**

126 **from presumed DCs showing membrane depolarizations (4.2 ± 0.3 mV, n = 8 cochleae) to successive periods of**

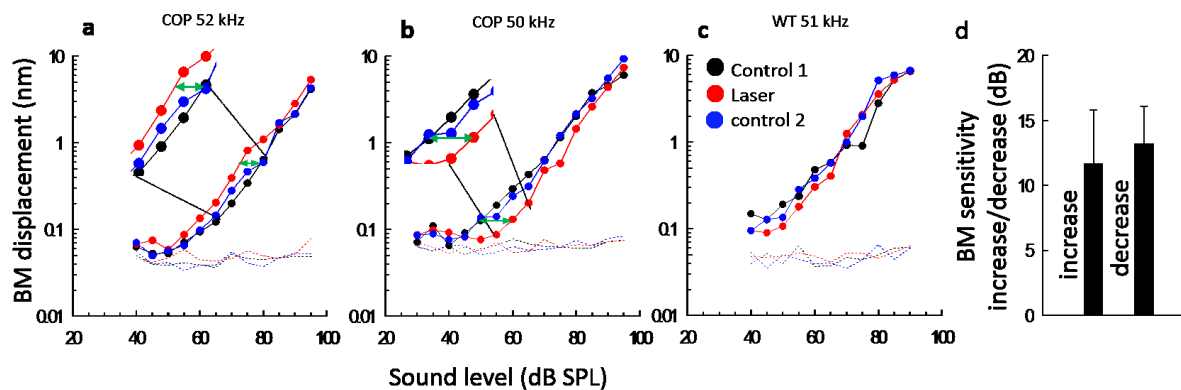
127 **BM laser illumination. (e) EP recorded from scala media during BM laser illumination. COP trace arrow: onset**

128 **step. WT littermate: nonresponsive to laser illumination. Blue bars in d and e: periods of 100 μ m diameter, 0.25**

129 **mWmm⁻², 470nm laser illumination.**

130

131 **Light-activation of COP-expressing supporting cells alters BM mechanical responses to**
132 **CF tone frequencies over their entire dynamic range.**



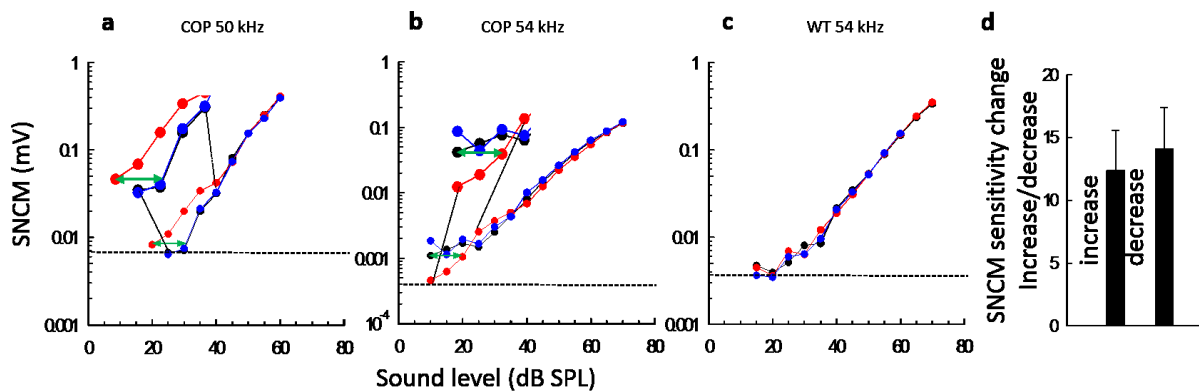
133

134 **Figure 3. BM Laser illumination alters the sensitivity of cochlear mechanical responses of COP mice over**
135 **their entire dynamic range. (a-c) BM displacement as functions of SPL from two COP (a,b) and one WT (c)**
136 **mice at the CF tone frequencies indicated. Measurements were, made before (black, control 1), during (red,**
137 **laser), and following (blue, control 2) BM laser illumination (see c). Dotted lines: measurement noise floors**
138 **Green arrows (a,b): maximum sensitivity change (expanded views: insets). d. Mean ±S.D of maximum**
139 **increases in sensitivity(11.7 ± 4.1 dB, $n = 7$ cochleae) and decreases (13.2 ± 2.9 dB, $n = 9$) of BM displacement**
140 **(green arrows a,b) during BM laser illumination in COP mice. There was no visible increase or decrease of BM**
141 **sensitivity in WT littermates (-1.3 ± 2.2 dB, $n = 6$ cochleae). Laser illumination: 100 mm beam diameter,**
142 **wavelength: 473 nm, power density = 0.25 mWmm^{-2} apart from $C = 0.75 \text{ mWmm}^{-2}$. All measurements from**
143 **different cochleae, uncompensated for middle-ear and electrode characteristics.**

144 To examine how light-activated COP-expressing supporting cells influence cochlear
145 mechanical sensitivity, we measured the dependence of BM displacement on sound pressure
146 level (SPL). Cochlear mechanical responses to CF and near CF tones are sensitive and
147 increase compressively with moderate to high SPL, indicating cochlear amplification². We
148 measured BM displacement level functions in response to CF and near CF tones from COP
149 mice (Fig. 3, a,b) and control littermates (WT, Fig. 3c) to discover if illumination of the BM
150 measurement site with a laser beam through the closed RW, in the 50kHz – 60 kHz, basal
151 region of the cochlea influenced BM level functions and hence cochlear sensitivity. BM laser

152 illumination in COP (Fig. 3a,b,d), but not WT littermates (Fig. 3c), caused reversible
 153 increases or reversible decreases in cochlear BM sensitivity throughout its dynamic range to
 154 tones at the CF of the recording site. The sensitivity changes occurred during BM
 155 illumination and returned to control levels within 35 - 70s after illumination. BM laser
 156 illumination of six WT littermates caused no measurable magnitude changes in BM level
 157 functions (Fig. 3c).

158 **Light-activation of COP-expressing supporting cells changes extracellular OHC tone-**
 159 **evoked electrical responses.**



160
 161 **Figure 4. BM Laser illumination alters the sensitivity of cochlear electrical responses that are subject to**
 162 **cochlear amplification in COP mice. (a-b)** Organ of Corti cochlear microphonic potential recorded from the
 163 SN (SNCM); magnitude as functions of SPL for sound stimulation at the CF frequencies indicated.
 164 Measurements made before (black), during (red), and following (blue) BM laser illumination (see 3c). Dotted
 165 lines: mean measurement noise floors. Green arrows: maximum sensitivity change (expanded views: insets). **d.**
 166 Mean \pm S.D of maximum increases in sensitivity (12.4 ± 3.2 dB, $n = 8$ cochleae) and decreases (14.1 ± 3.3 dB, n
 167 $= 7$) of SNCM (green arrows **a,b**) during BM laser illumination in COP mice. There was no visible increase or
 168 decrease of BM sensitivity in WT littermates (0.7 ± 1.8 dB, $n = 5$ cochleae). Laser illumination; 100 mm beam
 169 diameter, wavelength: 473 nm, **a,b**; power density = 0.25 mWmm^{-2} , C; = 0.75 mWmm^{-2} . All measurements
 170 from different cochleae, uncompensated for middle-ear and electrode characteristics.

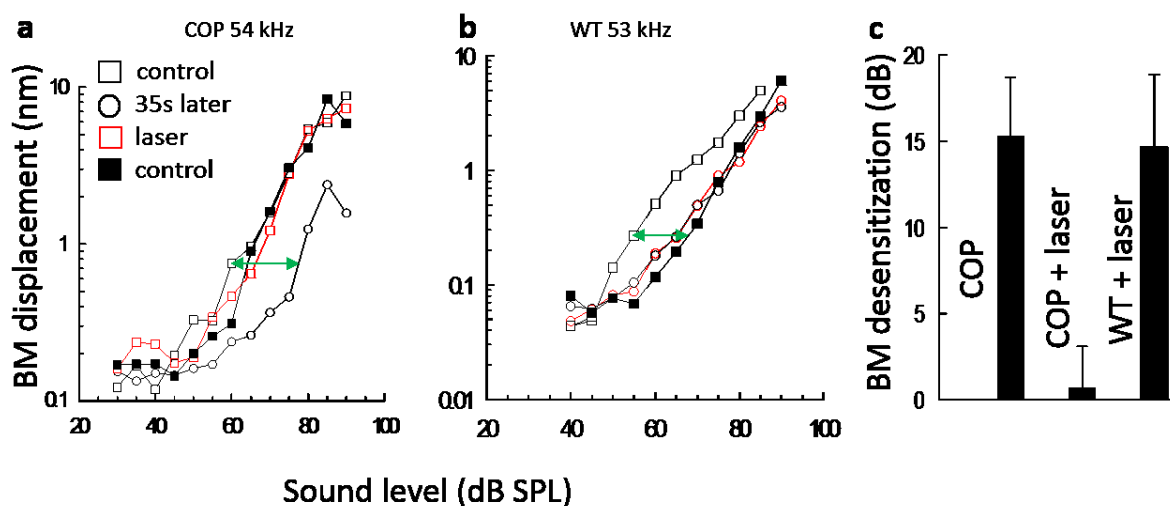
171

172 We measured the magnitude and phase of extracellular voltage responses or microphonic
173 potential recorded from the spaces of Nuel (SNCM) of the OC of COP and WT mice as a
174 function of SPL (level functions) in response to CF and near CF tones, with and without BM
175 illumination in the 50kHz – 60kHz region of the cochlea. Tone-evoked voltage responses
176 recorded in the OC vary considerably with the location of the recording site²². We found the
177 largest to be from the SN immediately adjacent to the OHCs and DCs. The SNCM is the
178 voltage produced across the resistive network of the SN²³ by the flow of the MET current,
179 dominated by K⁺ which flows outwards, down its electrochemical gradient, across the
180 basolateral membranes of the OHCs, where it accumulates in the fluid spaces of the OC²².
181 Excess K⁺ is “siphoned” by electro-neutral K/Cl co-transporters in the adjacent DCs^{24,25} and
182 cleared from the DC cytoplasm via an intercellular gap junctional pathway²⁶, thereby
183 preventing prolonged depolarization of the OHC membrane potential. At low-levels (0 – 40
184 dB SPL), SNCM is dominated by the amplified responses of OHCs to tones centered on the
185 cochlear frequency place of the measurement location. With increasing level above ~40 dB
186 SPL, OHCs from adjacent frequency regions contribute to the SNCM due to spread of
187 excitation²⁷. In 9 sensitive mice (CF thresholds 16.5 ±3.2 dB SPL), light-activation of DCs
188 and OPCs either increases and/or decreases (Fig. 4a,b,d) the sensitivity of SNCM responses
189 to CF and near CF tones for stimulus levels within ~30 dB SPL of threshold. Light activation
190 of DCs and OPCs had little influence on SNCM responses for levels above this. Sound-
191 evoked electrical responses recorded in the SN of five WT littermates to CF tones remained
192 unchanged by BM laser illumination, even when the laser power greatly exceeded the
193 threshold for COP-activation (Fig. 4c). Light-activation of COP-expressing DCs and OPCs
194 can, therefore, increase or decrease the mechanical responses of the BM to CF tones
195 throughout its dynamic range, but only influences OHC tone-evoked electrical responses to
196 levels that are subject to cochlear amplification (< 50 dB SPL).

197

198 **Light-activation of COP-expressing supporting cells accelerates sensory recovery of**
199 **temporarily desensitized cochleae.**

200 Brief exposure to loud sounds can temporarily desensitize the cochlea for seconds to minutes
201 ²⁸. Cochlear desensitization of about 15 dB (green arrows, Fig. 5a, b) occurred when the
202 required 5-minute recovery period between successive level function measurements, which
203 include high-level (80dB SPL) sound exposures, was omitted. Illumination of the BM in COP
204 (Fig. 5a, c), but not WT mice (Fig. 5b, c), eliminated the desensitizing shift between
205 measurements and cochlear sensitivity returned immediately to control levels.



206

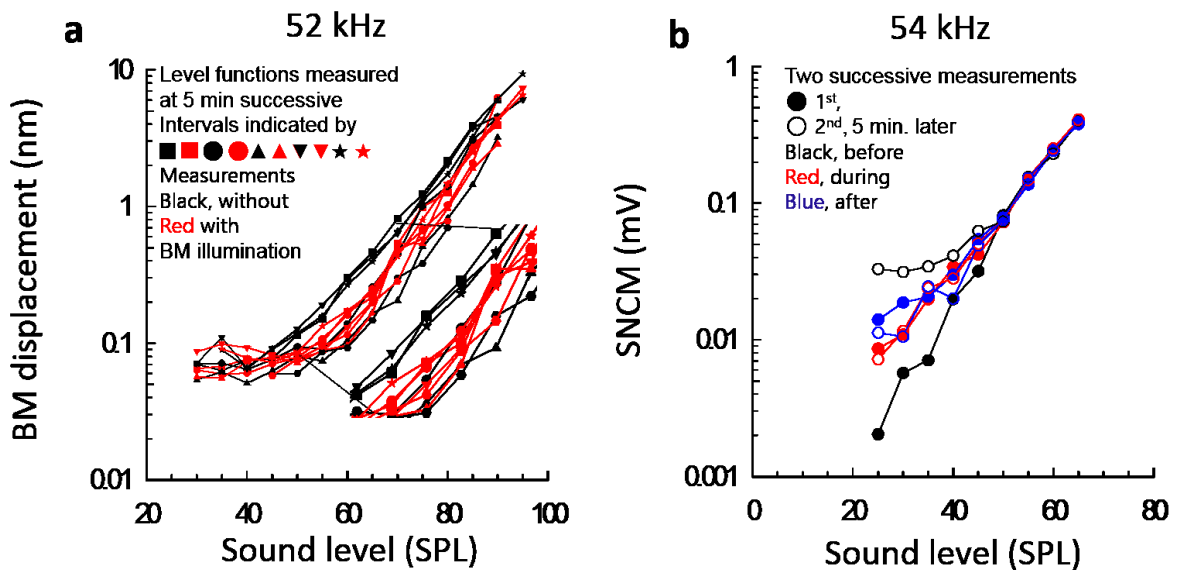
207 **Figure 5. BM Laser illumination of COP mice accelerates recovery of temporarily desensitized cochleae.**

208 **a:** BM displacement level functions measured in COP mouse in quick succession (35s intervals) after control
209 (open squares), without required 5-minute interval, becomes desensitized (open circles). Sensitivity returns
210 during the level run with BM laser illumination (red squares), measured 35s after the open circle level run.
211 Sensitivity is sustained during control level run (black solid squares), measured 35s after laser run. **b.** BM
212 displacement level functions measured in WT mouse using the same regime as for the COP mouse in **a.**
213 Maximum sensitivity change: green arrows (**a,b**). **c.** Bar graphs: maximum change in BM displacement
214 sensitivity to CF tone level functions presented successively in 35 ms intervals in COP mice without BM laser
215 illumination (15.3 ± 3.4 dB, $n = 6$ cochleae) and in COP (0.7 ± 2.4 dB, $n = 6$) and WT mice (14.7 ± 4.1 dB, $n =$

216 5) with laser illumination. Laser illumination: 100 mm beam diameter, wavelength: 473 nm, power density =
 217 0.25 mWmm^{-2} apart from $c = 0.75 \text{ mWmm}^{-2}$. All measurements uncompensated for middle-ear and electrode
 218 characteristics.

219 **A role for DCs and OPCs in controlling cochlear sensitivity.**

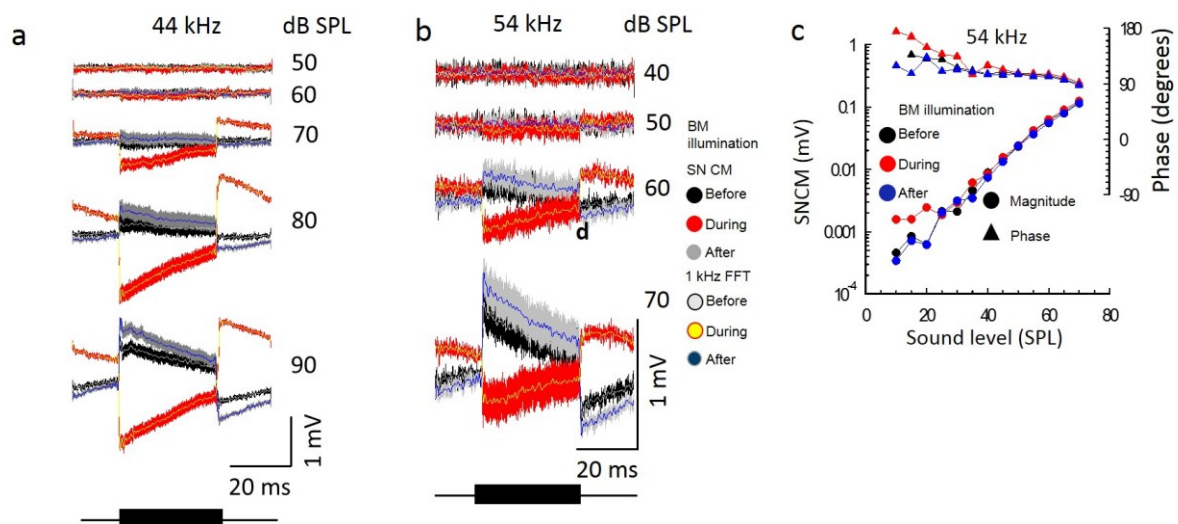
220 A role for supporting cells in controlling cochlear sensitivity became apparent in recordings
 221 from preparations with fluctuating sensitivity due to preceding high-SPL stimulation. The
 222 cochlear sensitivity fluctuated with a period of about 10 minutes and measurements were
 223 made at 5-minute intervals that fell in either hyper- or hyposensitivity phases. When these
 224 level functions were superimposed, responses measured during BM laser illumination tended
 225 to overlie each other regardless of whether BM illumination increased, or decreased the
 226 sensitivity of BM displacement and voltage response relative to the control measured just
 227 before each period of illumination (Fig. 6a, b). Light-activation of COP-expressing DCs and
 228 OPCs reduced the sensitivity of very sensitive BM responses and increased the sensitivity of
 229 BM responses during the transient desensitization phase. DCs and OPCs appeared to act as an
 230 active homeostatic system that returned cochlear sensitivity to a set level.



232 **Figure 6. OC supporting cells mediate homeostatic control of mechanical and electrical cochlear**
 233 **sensitivity. (a)** BM displacement level functions for CF tones, with expanded view (arrows), showing 10
 234 successive presentations (indicated by different symbols), measured at 5-minute intervals without and with BM
 235 laser illumination of a representative cochlea. **(b)** SNCM level functions for CF tones showing two successive
 236 presentations at 5-minute intervals measured during and following BM laser illumination, 473 nm, 0.25
 237 mWmm⁻².

238 **Light-activation of COP-expressing DCs and OPCs changes the polarity of the tonic**
 239 **component of the SNCM.**

240 During moderate to intense acoustic stimulation, the SNCM recorded in responses to near CF
 241 and CF tones develops a tonic, time-dependent, positive potential that increases with
 242 increasing SPL (Fig. 7a, b). For sound levels greater than about 70 dB SPL, the tonic
 243 component of the OCCM takes the form of a sharp depolarization of a few mV that declines
 244 over 10s of ms to zero mV, as has been reported previously²². At tone-offset, the SN
 245 becomes negative and recovers to zero over a time periods of 10s of



246
 247 **Figure 7. Light excitation of OC supporting cells changes the polarity of the tonic component of the**
 248 **OCCM in COP mice. (a,b)** Voltage responses (average of 20 presentations) to just below CF (44 kHz) and CF
 249 (54 kHz) tones recorded from the SN in different cochleae for the SPLs indicated before, during and after BM
 250 illumination. Superimposed traces: 1 kHz low-pass FFT filtered responses (tonic component of OCCM). **(c)**

251 SNCM magnitude and phase level functions for data in (b). BM laser illumination: 473 nm, 0.25 mWmm⁻². Bars
252 beneath traces indicate stimulating tone burst.

253 ms (Figs. 7a, b). These observations have been attributed to the accumulation and clearance
254 of K⁺ from the SN^{22,28}. BM illumination in COP mice caused the tonic component of the
255 SNCM to be reversed. The tonic component becomes a sharp, time-dependent negative
256 potential that becomes positive at tone offset, returning to zero potential over periods of 10s
257 of ms (Figs. 7a, b). Presumably, light-activation of the non-selective cation conductance of
258 COP-expressing DCs and OPCs, their consequent conductance increases and depolarization,
259 changes the properties of the electrical network of the OC²³. For levels above about 40 dB
260 SPL, however, the phase and magnitude of the SNCM remain unchanged (Fig. 7c), an
261 indication that the SNCM tonic potential polarity change does not influence OHC excitation.

262

263 **DISCUSSION**

264 The *in vivo* measurements reported here support the proposal that OHCs are enveloped by a
265 control system of specialized supporting cells that regulates passive and active mechanical
266 energy flow in the cochlea through sound-induced mechanical and electrochemical changes
267 in the OC. The mechanical and electrical changes we measured from the cochleae of COP
268 mice were initiated when the nonselective cation conductances expressed in DCs and OPCs
269 were gated by laser illumination, as demonstrated in *ex vivo* and *in vivo* electrophysiological
270 recording from single DCs (Fig. 2a-d). In this initial investigation, we demonstrated that
271 illumination increased the membrane conductance and depolarized the cells.

272 The earliest studies, using caged calcium in single cell preparations, revealed that DCs
273 exhibit Ca²⁺ dependent motility¹¹. Depolarization of DCs and OPCs could increase
274 intracellular Ca²⁺ levels due to influx through the gated COP channels and/or through ATP
275 mediated Ca²⁺ release from intracellular stores, as had been suggested for fast and slow Ca²⁺-

276 wave propagation in developing and adult DCs^{29,30}. This form of motility may underpin the
277 BM passive motility, which extends over the entire dynamic range of the BM sound-evoked
278 vibrations that we observe *in vivo*. Depolarization causes mechanical changes in the DCs that
279 include increases in the curvature of the DC phalangeal processes^{11,12,31} and increased turgor
280 pressure³¹. Mechanical changes in DCs cause changes in the turgor pressure of isolated
281 OHCs, which modulates OHC electromotility and is predicted to modulate cochlear
282 amplification^{31,32}, which is what we have observed here. However, perhaps more significant,
283 but yet to be investigated, is that in parallel with changes in OHC electro-mechanical
284 sensitivity³¹, changes to the mechanical properties of the DCs and OPCs alters impedance
285 matching between the OHCs and their supporting cell scaffold³³. Similar effects *in vivo*
286 could account for our finding that, while OHC voltage responses to CF and near CF tones are
287 sensitive to COP light activation only over those levels that are susceptible to cochlear
288 amplification, BM displacements are sensitive to light activation over their entire dynamic
289 range and at levels and frequencies that have no observable influence on magnitude and
290 phase of OHC SNCM. These findings appear to indicate that these DC and OPC can induce
291 mechanical changes in the cochlear partition which do not influence OHC MET. However,
292 lack of observable effect of light activation on SNCM at higher stimulus levels may be due to
293 summation and cancelation effects because of spread of the OC electrical potentials with
294 increasing stimulus level (e.g.³⁴).

295 We also observed that light activated conductance changes in DCs and OPCs reduced the EP.
296 The initial effect, which was to reduce the EP by about a millivolt, is likely due to light
297 activated gating of the COP channels. The long-term slow effect that commenced 1-3 s after
298 the initial EP reduction reduced the EP by around 20 mV. The basis of this long-term
299 reduction requires further investigation but could involve the gap junctions that interconnect
300 supporting cells of the OC, purinergic excitation and Ca²⁺-signaling^{35,36}. Furthermore, a

301 ~20% reduction in EP (Fig. 2e) has little influence on OHC extracellular voltage responses
302 recorded from the OC, as has been reported previously^{14,37}.

303 The mouse cochlea, especially the high frequency region, is susceptible to temporary
304 desensitization, which is also observed in guinea pigs³⁸. For this reason, several minutes
305 were left between each level run measurement. If these were missed, the cochlear became
306 desensitized and only returned to full sensitivity after 5 minutes rest. Illumination of the BM
307 in COP, but not wild type mice, restored sensitivity almost immediately. It appears that
308 depolarization of DCs and OPCs accelerates recovery from desensitization.

309 When exposed to a train of moderately loud tones at a frequency about a half octave below
310 the CF, OHCs slowly become increasingly depolarized over time during the presentation of a
311 train of tones³⁸. By contrast, the OC NS becomes sharply depolarized at tone onset, which
312 declines over time and results in hyperpolarization at tone offset and recovers over time as
313 revealed by²² and confirmed by SN measurements reported here. The loud tones were
314 suggested to cause cytoplasmic accumulation of K^+ , which depolarized the OHCs and
315 travelled down its concentration gradient across the OHC basolateral membranes into the SN
316⁷. Following hair cell transduction, the resting perilymphatic $[K^+]$ is raised locally by several
317 mM²², which is syphoned away by electro-neutral K^+/Cl^- co-transporters in the adjacent DCs
318^{24,25}, thereby preventing prolonged depolarization of the OHC membrane potential. This
319 transport mechanism is presumed to be facilitated by a constant clearance of K^+ from the DC
320 cytoplasm via an intercellular gap junctional pathway²⁶. The different time courses of K^+
321 accumulation and removal in OHCs and the SN might be expected to result in time-
322 dependent driving voltages for generating the time-varying amplitudes of the tonic (DC)
323 components of the intracellular OHC receptor potential and extracellular SNCM.
324 Nevertheless, the kinetics of these processes for high level and/or prolonged acoustic
325 stimulation results in cochlear desensitization because the DCs and OPCs are not able to

326 remove K^+ quickly enough. Light activation of the non-selective cation channels expressed in
327 the DCs and OPCs of COP mice and consequent DC and OPC depolarization overcomes this
328 desensitization, presumably by increasing the ability of DCs and OPCs to buffer and recycle
329 K^+ at a faster rate. DCs have resting membrane potentials more negative than -100 mV,
330 which is more negative than the expected equilibrium potential of K^+ in the SN, and the OHC
331 cytoplasm. When the COP channels are gated, K^+ would be expected to flow down this steep
332 electrochemical gradient into the DCs and OPCs, which might account for the changed
333 polarity of the tonic component of the SNCM during BM illumination. Regardless of the
334 mechanism, the gating of non-selective cation channels in DCs and OPCs reduces the period
335 of cochlear insensitivity following a loud tone.

336 Fluctuations in cochlear sensitivity (Fig. 6) provides evidence that OHCs and their closely
337 associated supporting cells interact continuously to make fine adjustments to hearing
338 sensitivity, possibly due to tone induced fluctuations in extracellular K^+ ²². Light activation of
339 nonselective cation channels and the consequent rapid shunting of K^+ effectively shunts this
340 interaction and the system settles to a quiescent steady state (Fig. 6), presumably by
341 minimizing the SN K^+ levels. This finding may provide a basis for why a higher density of
342 cation channels is not normally expressed in DCs and OPCs. When activated in COP mice,
343 their increased conductance effectively short-circuits the mechanism that fine controls
344 cochlear sensitivity. Another reason for the limited K^+ buffering abilities of supporting cells
345 might originate from apparent lack of selective evolutionary pressure that favors the
346 expression of such a system that ensures rapid recovery from temporary threshold shift
347 because acoustic stimulation, which causes temporary threshold shift, is virtually absent in
348 natural animal habitats.

349 Further studies are clearly required to fully elucidate the mechanisms by which OC
350 supporting cells control the mechanical, electrical and ionic environment of the OHCs. These

351 studies are essential for understanding the normal function of OC supporting cells in cochlear
352 sensory processing. Their role should not be ignored in the challenge to restore hearing
353 function by repairing and regenerating sensory hair cells. Optogenetics, in its different forms,
354 could offer new opportunities in both the investigation of normal and abnormal function in
355 the cochlea and its eventual treatment.

356

357 **Acknowledgements:**

358 The authors thank Sarath Vijayakumar and Cassidy Nguyen for technical assistance on
359 mouse colony management at Creighton University, and Milos Stankovic for assistance with
360 Figure 1A.

361 **Funding:** This work was funded by the Medical Research Council (grant MR/ N004299/1).

362 **Author contributions:** IJR, ANL and JZ, conceived and designed the study. JZ designed
363 mice with ChR expressing cochlear supporting cells. JAD designed ChR mouse cross
364 experiments and contributed to genotyping. SL designed *ex vivo* measurements. ANL and IJR
365 designed *in vivo* measurements. PS and SL measured and analyzed data from *ex vivo*
366 experiments. VAL and IJR measured and analyzed data from *in vivo* experiments. SL
367 prepared cochleae for immunohistochemistry and ZX performed cochlear
368 immunohistochemistry. VAL organized mouse breeding at Brighton. ANL wrote computer
369 programs. IJR and ANL wrote the paper with contributions from the other authors.

370 **Competing interests:** Authors declare no competing interests.

371 **Data and materials availability:** All data is available in the main text or the supplementary
372 materials. Additional data related to this paper may be requested from the authors.

373 **Supplementary Materials**

374 Materials and Methods

375 **References**

- 376 1 Lim, D. J. Functional structure of the organ of Corti: a review. *Hearing Res.* **22**, 117-
377 146, doi:10.1016/0378-5955(86)90089-4 (1986).
- 378 2 Robles, L. & Ruggero, M. A. Mechanics of the Mammalian Cochlea. *Physiol. Rev.*
379 **81**, 1305-1352 (2001).
- 380 3 Brownell, W. E., Bader, C. R., Bertrand, D. & de Ribaupierre, Y. Evoked mechanical
381 responses of isolated cochlear outer hair cells. *Science* **227**, 194-196 (1985).
- 382 4 Ashmore, J. F. A fast motile response in guinea-pig outer hair cells: the cellular basis
383 of the cochlear amplifier. *The Journal of Physiology* **388**, 323-347 (1987).
- 384 5 Santos-Sacchi, J. & Dilger, J. P. Whole cell currents and mechanical responses of
385 isolated outer hair cells. *Hearing Res.* **35**, 143-150, doi:[https://doi.org/10.1016/0378-
386 5955\(88\)90113-X](https://doi.org/10.1016/0378-5955(88)90113-X) (1988).
- 387 6 Corey, D. P. & Hudspeth, A. J. Ionic basis of the receptor potential in a vertebrate hair
388 cell. *Nature* **281**, 675-677 (1979).
- 389 7 Russell, I. J. Origin of the receptor potential in inner hair cells of the mammalian
390 cochlea--evidence for Davis' theory. *Nature* **301**, 334-336, doi:10.1038/301334a0
391 (1983).
- 392 8 Dallos, P. Cochlear amplification, outer hair cells and prestin. *Curr. Opin. Neurobiol.*
393 **18**, 370-376, doi:10.1016/j.conb.2008.08.016 (2008).
- 394 9 Flock, Å., Flock, B., Fridberger, A., Scarfone, E. & Ulfendahl, M. Supporting Cells
395 Contribute to Control of Hearing Sensitivity. *The Journal of Neuroscience* **19**, 4498-
396 4507 (1999).
- 397 10 Jacob, S., Johansson, C. & Fridberger, A. Noise-induced alterations in cochlear
398 mechanics, electromotility, and cochlear amplification. *Pflügers Archiv - European
399 Journal of Physiology* **465**, 907-917, doi:10.1007/s00424-012-1198-4 (2012).
- 400 11 Dulon, D., Blanchet, C. & Laffon, E. Photoreleased Intracellular Ca²⁺ Evokes
401 Reversible Mechanical Responses in Supporting Cells of the Guinea-Pig Organ of
402 Corti. *Biochem. Biophys. Res. Commun.* **201**, 1263-1269,
403 doi:<https://doi.org/10.1006/bbrc.1994.1841> (1994).
- 404 12 Bobbin, R. P. ATP-induced movement of the stalks of isolated cochlear Deiters' cells.
405 *Neuroreport* **12**, 2923-2926 (2001).

- 406 13 Lagostena, L., Cicuttin, A., Inda, J., Kachar, B. & Mammano, F. Frequency
407 Dependence of Electrical Coupling in Deiters' Cells of the Guinea Pig Cochlea. *Cell*
408 *Communication & Adhesion* **8**, 393-399, doi:10.3109/15419060109080760 (2001).
- 409 14 Lukashkina, V. A., Levic, S., Lukashkin, A. N., Strenzke, N. & Russell, I. J. A
410 connexin30 mutation rescues hearing and reveals roles for gap junctions in cochlear
411 amplification and micromechanics. *Nature Communications* **8**, 14530,
412 doi:10.1038/ncomms14530 (2017).
- 413 15 Parsa, A., Webster, P. & Kalinec, F. Deiters cells tread a narrow path—The Deiters
414 cells-basilar membrane junction—. *Hearing Res.* **290**, 13-20,
415 doi:<https://doi.org/10.1016/j.heares.2012.05.006> (2012).
- 416 16 Motallebzadeh, H., Soons, J. A. M. & Puria, S. Cochlear amplification and tuning
417 depend on the cellular arrangement within the organ of Corti. *Proceedings of the*
418 *National Academy of Sciences* **115**, 5762-5767, doi:10.1073/pnas.1720979115 (2018).
- 419 17 Cox, B. C., Liu, Z., Lagarde, M. M. M. & Zuo, J. Conditional Gene Expression in the
420 Mouse Inner Ear Using Cre-loxP. *JARO* **13**, 295-322, doi:10.1007/s10162-012-0324-
421 5 (2012).
- 422 18 Walters, B. J. *et al.* In Vivo Interplay between p27Kip1, GATA3, ATOH1, and
423 POU4F3 Converts Non-sensory Cells to Hair Cells in Adult Mice. *Cell Reports* **19**,
424 307-320, doi:<https://doi.org/10.1016/j.celrep.2017.03.044> (2017).
- 425 19 Hayashi, T., Ray, C. A., Younkins, C. & Bermingham-McDonogh, O. Expression
426 patterns of FGF receptors in the developing mammalian cochlea. *Dev. Dyn.* **239**,
427 1019-1026, doi:10.1002/dvdy.22236 (2010).
- 428 20 Nagel, G. *et al.* Channelrhodopsin-1: A Light-Gated Proton Channel in Green Algae.
429 *Science* **296**, 2395-2398, doi:10.1126/science.1072068 (2002).
- 430 21 Nagel, G. *et al.* Channelrhodopsin-2, a directly light-gated cation-selective membrane
431 channel. *Proceedings of the National Academy of Sciences* **100**, 13940-13945,
432 doi:10.1073/pnas.1936192100 (2003).
- 433 22 Johnstone, B. M., Patuzzi, R., Syka, J. & Syková, E. Stimulus-related potassium
434 changes in the organ of Corti of guinea-pig. *The Journal of Physiology* **408**, 77-92,
435 doi:10.1113/jphysiol.1989.sp017448 (1989).
- 436 23 Mistrik, P. & Ashmore, J. F. Reduced Electromotility of Outer Hair Cells Associated
437 with Connexin-Related Forms of Deafness: An In silico Study of a Cochlear Network
438 Mechanism. *JARO* **11**, 559-571, doi:10.1007/s10162-010-0226-3 (2010).

- 439 24 Boettger, T. *et al.* Deafness and renal tubular acidosis in mice lacking the K-Cl co-
440 transporter Kcc4. *Nature* **416**, 874-878, doi:10.1038/416874a (2002).
- 441 25 Boettger, T. *et al.* Loss of K-Cl co-transporter KCC3 causes deafness,
442 neurodegeneration and reduced seizure threshold. *The EMBO Journal* **22**, 5422-5434,
443 doi:10.1093/emboj/cdg519 (2003).
- 444 26 Jagger, D. J. & Forge, A. Compartmentalized and Signal-Selective Gap Junctional
445 Coupling in the Hearing Cochlea. *The Journal of Neuroscience* **26**, 1260-1268,
446 doi:10.1523/jneurosci.4278-05.2006 (2006).
- 447 27 Cheatham, M., Naik, K. & Dallos, P. Using the Cochlear Microphonic as a Tool to
448 Evaluate Cochlear Function in Mouse Models of Hearing. *JARO - Journal of the*
449 *Association for Research in Otolaryngology* **12**, 113-125, doi:10.1007/s10162-010-
450 0240-5 (2011).
- 451 28 Cody, A. R. & Russell, I. J. Acoustically induced hearing loss: Intracellular studies in
452 the guinea pig cochlea. *Hearing Res.* **35**, 59-70, doi:10.1016/0378-5955(88)90040-8
453 (1988).
- 454 29 Tritsch, N. X., Yi, E., Gale, J. E., Glowatzki, E. & Bergles, D. E. The origin of
455 spontaneous activity in the developing auditory system. *Nature* **450**, 50-55,
456 doi:10.1038/nature06233 (2007).
- 457 30 Sirko, P., Gale, J. E. & Ashmore, J. F. Intercellular Ca²⁺ signalling in the adult
458 mouse cochlea. *The Journal of Physiology* **597**, 303-317, doi:10.1113/jp276400
459 (2019).
- 460 31 Yu, N. & Zhao, H.-B. Modulation of Outer Hair Cell Electromotility by Cochlear
461 Supporting Cells and Gap Junctions. *PLoS ONE* **4**, e7923,
462 doi:10.1371/journal.pone.0007923 (2009).
- 463 32 Kakehata, S. & Santos-Sacchi, J. Membrane tension directly shifts voltage
464 dependence of outer hair cell motility and associated gating charge. *Biophys. J.* **68**,
465 2190-2197, doi:[https://doi.org/10.1016/S0006-3495\(95\)80401-7](https://doi.org/10.1016/S0006-3495(95)80401-7) (1995).
- 466 33 Ramamoorthy, S. & Nuttall, Alfred L. Outer Hair Cell Somatic Electromotility
467 In Vivo and Power Transfer to the Organ of Corti. *Biophys. J.* **102**, 388-398,
468 doi:10.1016/j.bpj.2011.12.040 (2012).
- 469 34 Fridberger, A. *et al.* Organ of Corti Potentials and the Motion of the Basilar
470 Membrane. *The Journal of Neuroscience* **24**, 10057-10063,
471 doi:10.1523/jneurosci.2711-04.2004 (2004).

- 472 35 Lagostena, L. & Mammano, F. Intracellular calcium dynamics and membrane
473 conductance changes evoked by Deiters' cell purinoceptor activation in the organ of
474 Corti. *Cell Calcium* **29**, 191-198, doi:<https://doi.org/10.1054/ceca.2000.0183> (2001).
- 475 36 Thorne, P. R., Muñoz, D. J. B. & Housley, G. D. Purinergic Modulation of Cochlear
476 Partition Resistance and Its Effect on the Endocochlear Potential in the Guinea Pig.
477 *JARO* **5**, 58-65, doi:10.1007/s10162-003-4003-4 (2004).
- 478 37 Wang, Y., Fallah, E. & Olson, E. S. Adaptation of Cochlear Amplification to Low
479 Endocochlear Potential. *Biophys. J.* **116**, 1769-1786,
480 doi:<https://doi.org/10.1016/j.bpj.2019.03.020> (2019).
- 481 38 Cody, A. R. & Russell, I. J. Outer hair cells in the mammalian cochlea and noise-
482 induced hearing loss. *Nature* **315**, 662-665 (1985).

483

484 Supplementary Materials only:

- 485 1 Cox, B. C., Liu, Z., Lagarde, M. M. M. & Zuo, J. Conditional Gene Expression in the
486 Mouse Inner Ear Using Cre-loxP. *JARO* **13**, 295-322, doi:10.1007/s10162-012-0324-
487 5 (2012).
- 488 2 Walters, B. J. et al. In Vivo Interplay between p27Kip1, GATA3, ATOH1, and
489 POU4F3 Converts Non-sensory Cells to Hair Cells in Adult Mice. *Cell Reports* **19**,
490 307-320, doi:<https://doi.org/10.1016/j.celrep.2017.03.044> (2017).
- 491 3 Legan, P. K. et al. A Targeted Deletion in [alpha]-Tectorin Reveals that the Tectorial
492 Membrane Is Required for the Gain and Timing of Cochlear Feedback. *Neuron* **28**,
493 273-285, doi:10.1016/s0896-6273(00)00102-1 (2000).
- 494 4 Wu, T. et al. Optogenetic Control of Mouse Outer Hair Cells. *Biophys. J.* **110**, 493-
495 502, doi:<http://dx.doi.org/10.1016/j.bpj.2015.11.3521> (2016).
- 496 5 Zhang, F., Wang, L.-P., Boyden, E. S. & Deisseroth, K. Channelrhodopsin-2 and
497 optical control of excitable cells. *Nat. Methods* **3**, 785-792, doi:10.1038/nmeth936
498 (2006).

499 6 Aravanis, A. M. et al. An optical neural interface:in vivocontrol of rodent motor
500 cortex with integrated fiberoptic and optogenetic technology. Journal of Neural
501 Engineering 4, S143-S156, doi:10.1088/1741-2560/4/3/s02 (2007).

502 7 Lukashkin, A. N., Bashtanov, M. E. & Russell, I. J. A self-mixing laser-diode
503 interferometer for measuring basilar membrane vibrations without opening the
504 cochlea. J. Neurosci. Methods 148, 122-129, doi:10.1016/j.jneumeth.2005.04.014
505 (2005).

506

Figures

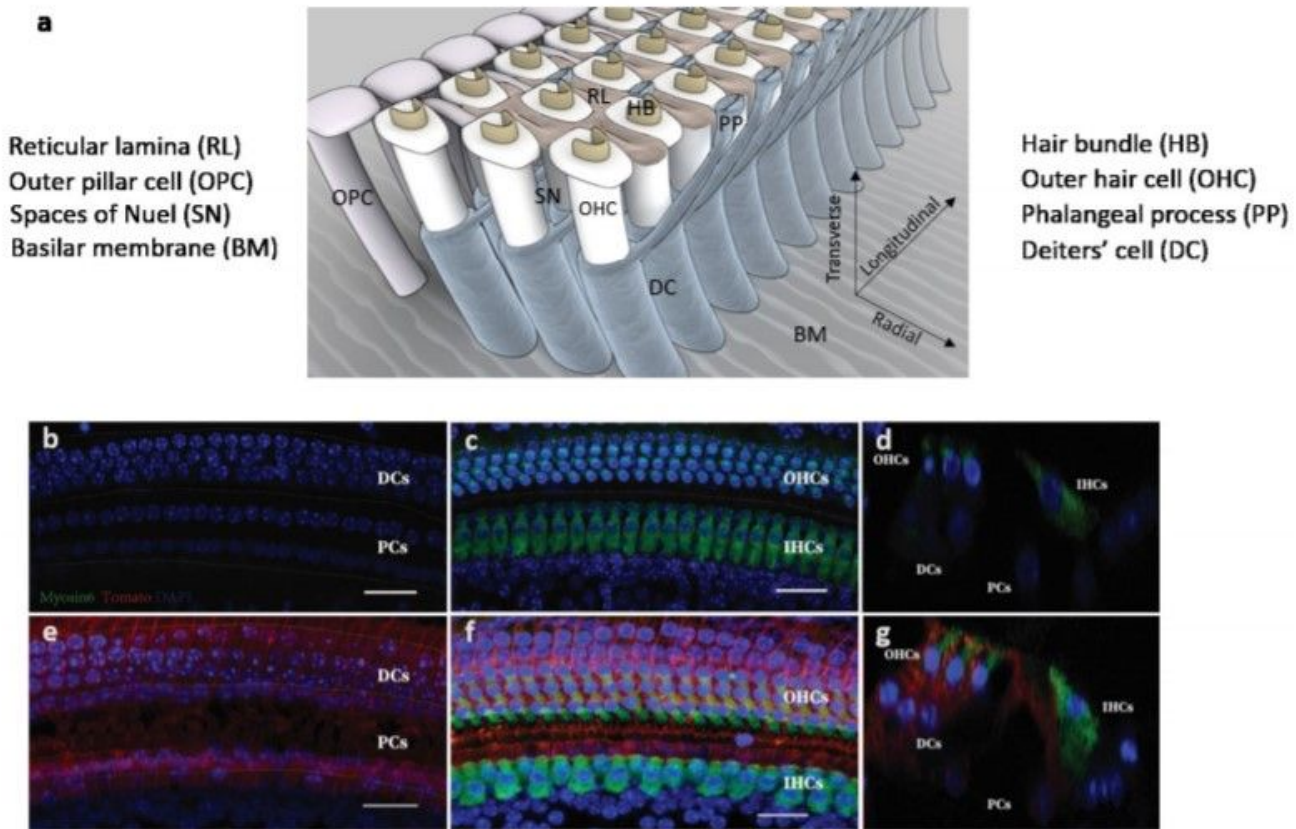


Figure 1

Schematic of the organ of Corti and expression of COP-tdTomato ChR in its supporting cells. (a) Schematic of the radially distal region of the organ of Corti. (b-g) ChR expression in the DCs and inner and outer pillar cells (PCs). *Fgfr3-iCreERT2*; COP-tdTomato mice were induced with tamoxifen (TMX) at P12/13 and analyzed at postnatal-day 28. (b-d) *Fgfr3-iCreERT2*^{-/-}; COP-tdTomato⁺ control mice. (e-g) *Fgfr3-iCreERT2*⁺; COPtdTomato⁺ experimental mice. (b,c,e,f) wholemount cochlear basal turns. (b,e) supporting cell layers. (c,f) projections of supporting cell and hair cell layers. (d,g) optical cross-sections in (b,c) and (e,f) respectively. IHCs: inner hair cells. Green: Myo6; blue: DAPI; red: autofluorescence of tdTomato. Scale bar = 20um.

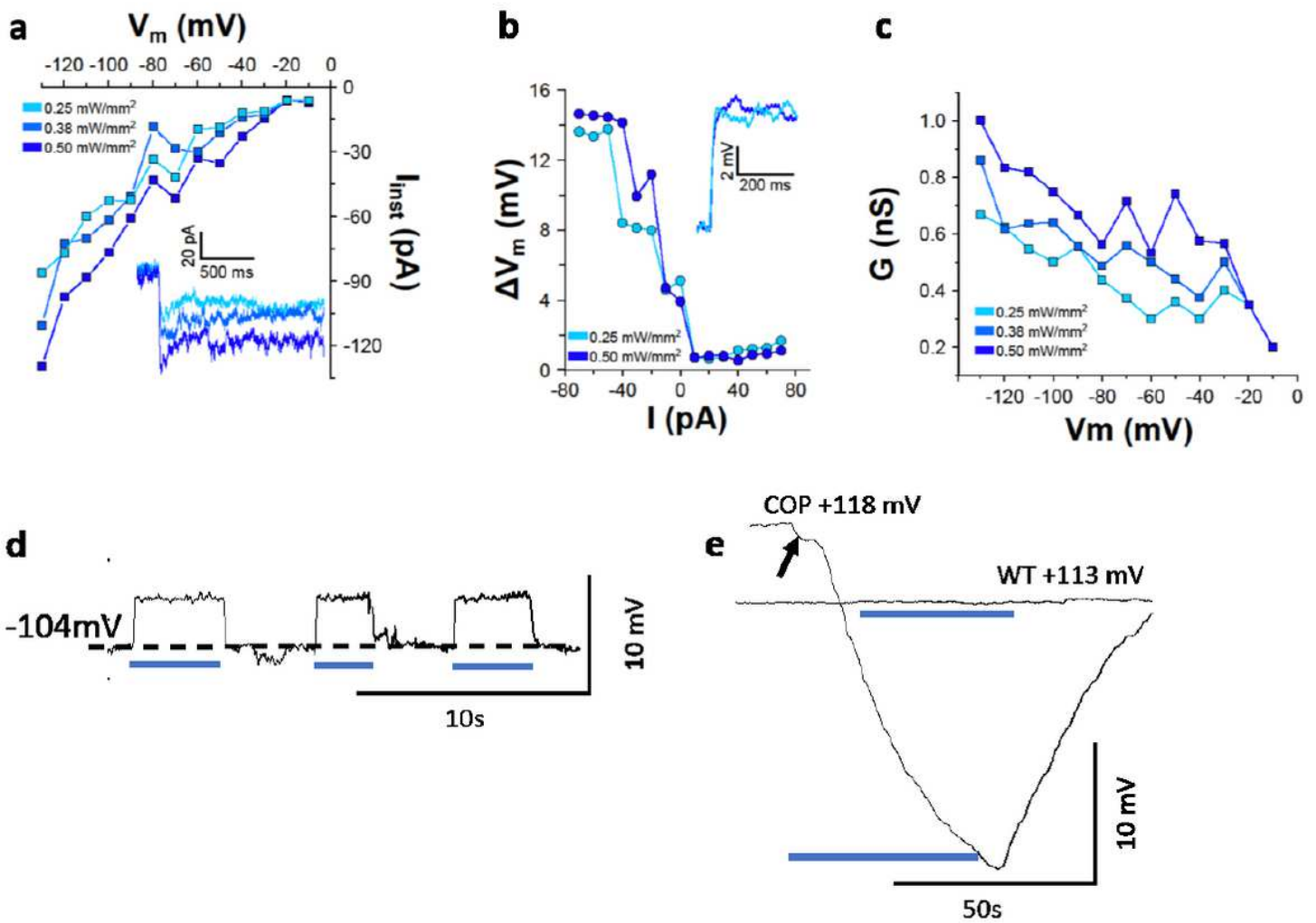


Figure 2

Cochlear illumination depolarizes COP mouse DC membrane potentials and reduces the endocochlear potential. (a) Ex vivo whole-cell patch recordings of current-voltage (I - V) plot: peak current amplitudes of a DC elicited in response to laser illumination at different power densities, as functions of membrane potential. Inset: Inward current traces at different laser power densities (-90 mV holding potential). (b) Ex vivo light-induced potential-current (ΔV - I) relationship of a DC: membrane potential changes (ΔV) during laser illumination as functions of injected currents. Light-induced depolarizations were elicited during negative current injection. Inset: whole-cell current-clamp recording (resting membrane potential = -50 mV) of light elicited depolarization with different laser power densities. (c) Conductance G (nS) as a function of membrane potential V (mV) at 3 different laser power densities using data in (a) at -130 mV holding potential. Increasing laser power increased the DC membrane conductance (0.67 , 0.86 and 1 nS respectively). (d) In vivo intracellular recordings from presumed DCs showing membrane depolarizations (4.2 ± 0.3 mV, $n = 8$ cochleae) to successive periods of BM laser illumination. (e) EP recorded from scala media during BM laser illumination. COP trace arrow: onset step. WT littermate: nonresponsive to laser illumination. Blue bars in d and e: periods of $100 \mu\text{m}$ diameter, 0.25 mW/mm^2 , 470nm laser illumination.

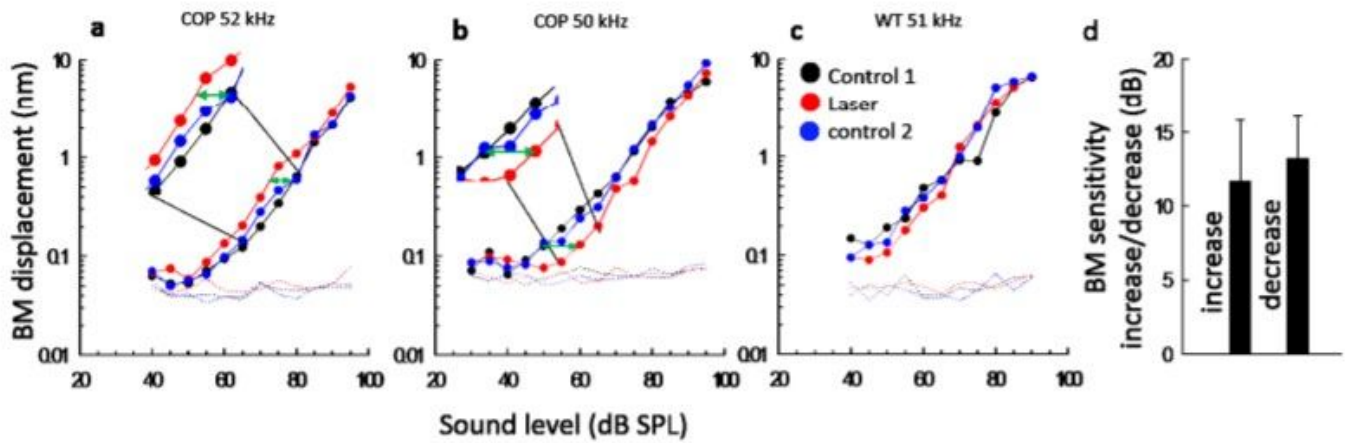


Figure 3

BM Laser illumination alters the sensitivity of cochlear mechanical responses of COP mice over their entire dynamic range. (a-c) BM displacement as functions of SPL from two COP (a,b) and one WT (c) mice at the CF tone frequencies indicated. Measurements were, made before (black, control 1), during (red, laser), and following (blue, control 2) BM laser illumination (see c). Dotted lines: measurement noise floors Green arrows (a,b): maximum sensitivity change (expanded views: insets). d. Mean \pm S.D of maximum 139 increases in sensitivity (11.7 ± 4.1 dB, $n = 7$ cochleae) and decreases (13.2 ± 2.9 dB, $n = 9$) of BM displacement (green arrows a,b) during BM laser illumination in COP mice. There was no visible increase or decrease of BM sensitivity in WT littermates (-1.3 ± 2.2 dB, $n = 6$ cochleae). Laser illumination: 100 mm beam diameter, wavelength: 473 nm, power density = 0.25 mWmm⁻² apart from C = 0.75 mWmm⁻² 142. All measurements from different cochleae, uncompensated for middle-ear and electrode characteristics.

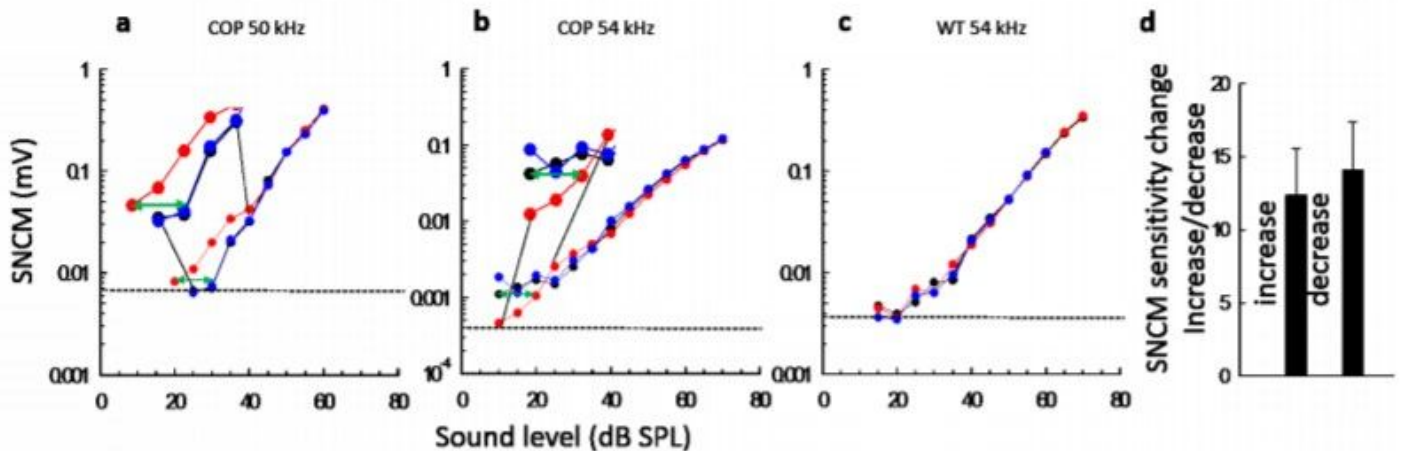


Figure 4

BM Laser illumination alters the sensitivity of cochlear electrical responses that are subject to cochlear amplification in COP mice. (a-b) Organ of Corti cochlear microphonic potential recorded from the SN (SNCM); magnitude as functions of SPL for sound stimulation at the CF frequencies indicated. Measurements made before (black), during (red), and following (blue) BM laser illumination (see 3c). Dotted lines: mean measurement noise floors. Green arrows: maximum sensitivity change (expanded views: insets). d. Mean \pm S.D of maximum increases in sensitivity (12.4 ± 3.2 dB, $n = 8$ cochleae) and decreases (14.1 ± 3.3 dB, $n = 7$) of SNCM (green arrows a,b) during BM laser illumination in COP mice. There was no visible increase or decrease of BM sensitivity in WT littermates (0.7 ± 1.8 dB, $n = 5$ cochleae). Laser illumination; 100 mm beam diameter, wavelength: 473 nm, a,b; power density = 0.25 mWmm^{-2} , C; = 0.75 mWmm^{-2} 169 . All measurements from different cochleae, uncompensated for middle-ear and electrode characteristics.

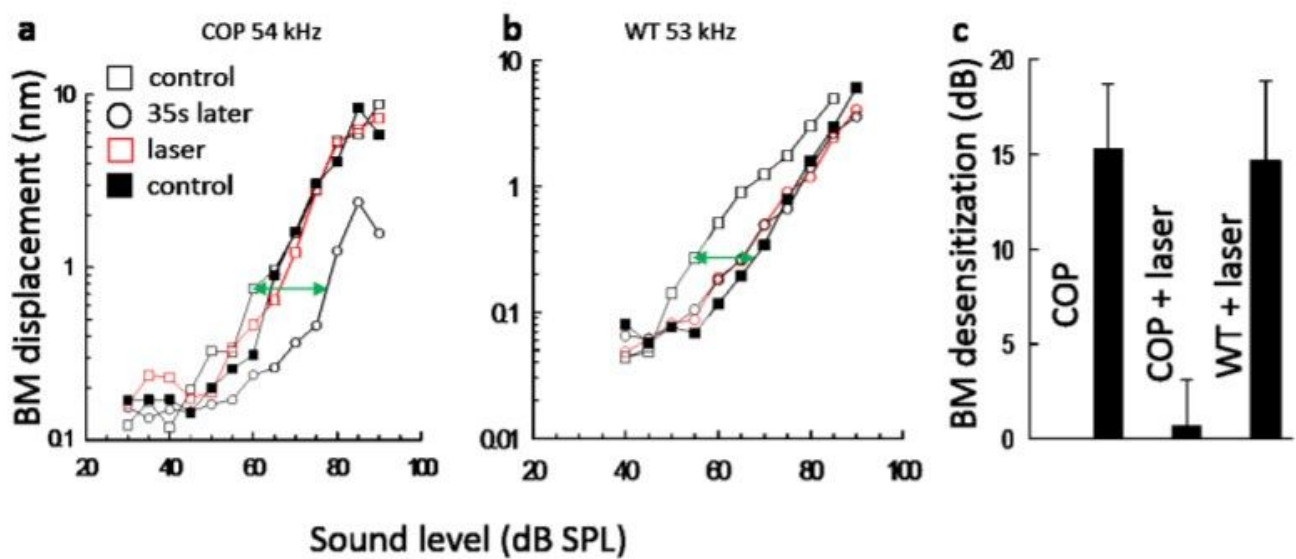


Figure 5

BM Laser illumination of COP mice accelerates recovery of temporarily desensitized cochleae. a: BM displacement level functions measured in COP mouse in quick succession (35s intervals) after control (open squares), without required 5-minute interval, becomes desensitized (open circles). Sensitivity returns during the level run with BM laser illumination (red squares), measured 35s after the open circle level run. Sensitivity is sustained during control level run (black solid squares), measured 35s after laser run. b. BM displacement level functions measured in WT mouse using the same regime as for the COP mouse in a. Maximum sensitivity change: green arrows (a,b). c. Bar graphs: maximum change in BM displacement sensitivity to CF tone level functions presented successively in 35 ms intervals in COP mice without BM laser illumination (15.3 ± 3.4 dB, $n = 6$ cochleae) and in COP (0.7 ± 2.4 dB, $n = 6$) and WT mice (14.7 ± 4.1 dB, $n = 5$) with laser illumination. Laser illumination: 100 mm beam diameter, wavelength: 473 nm, power density = 0.25 mWmm^{-2} apart from c = 0.75 mWmm^{-2} 217 . All measurements uncompensated for middle-ear and electrode characteristics.

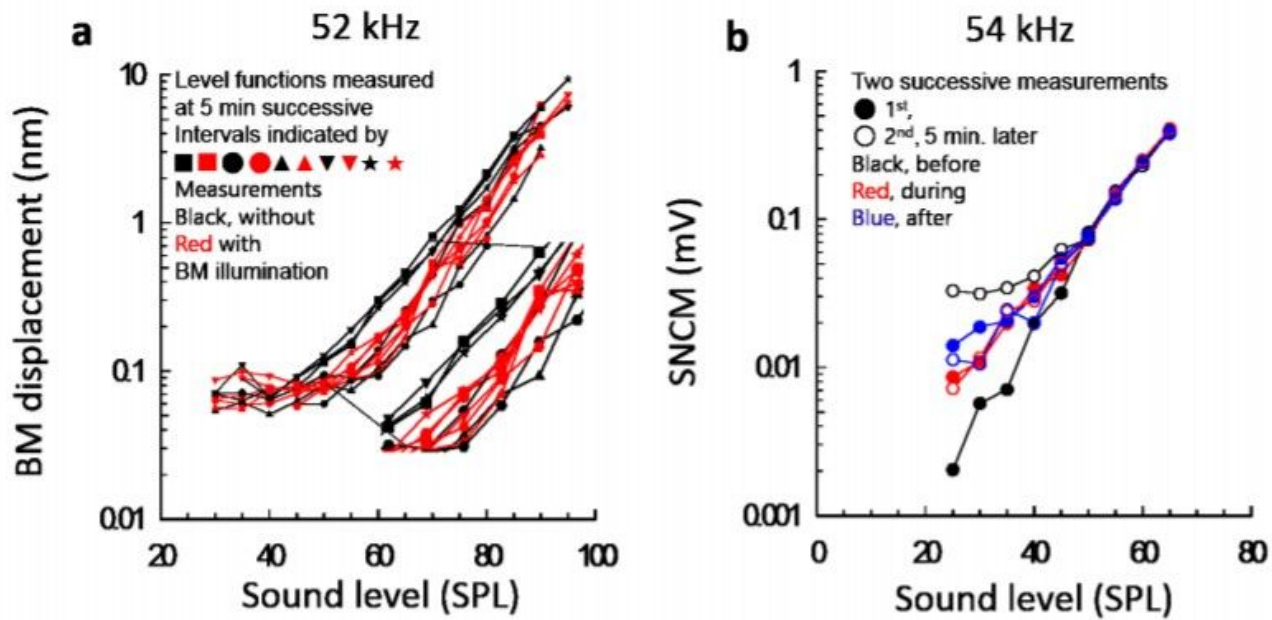


Figure 6

OC supporting cells mediate homeostatic control of mechanical and electrical cochlear sensitivity. (a) BM displacement level functions for CF tones, with expanded view (arrows), showing 10 successive presentations (indicated by different symbols), measured at 5-minute intervals without and with BM laser illumination of a representative cochlea. (b) SNCM level functions for CF tones showing two successive presentations at 5-minute intervals measured during and following BM laser illumination, 473 nm, 0.25 mWmm⁻²

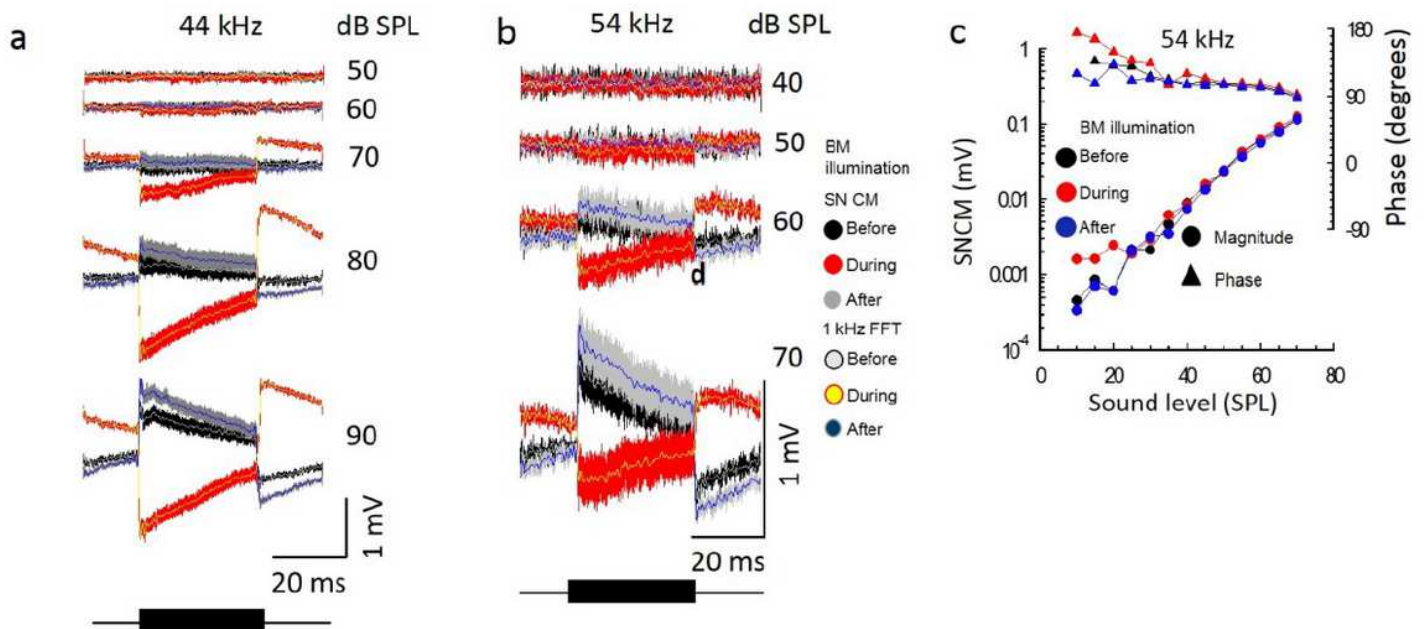


Figure 7

Light excitation of OC supporting cells changes the polarity of the tonic component of the OCCM in COP mice. (a,b) Voltage responses (average of 20 presentations) to just below CF (44 kHz) and CF (54 kHz) tones recorded from the SN in different cochleae for the SPLs indicated before, during and after BM illumination. Superimposed traces: 1 kHz low-pass FFT filtered responses (tonic component of OCCM). (c) SNCM magnitude and phase level functions for data in (b). BM laser illumination: 473 nm, 0.25 mWmm⁻² 251 . Bars beneath traces indicate stimulating tone burst.

Supplementary Files

This is a list of supplementary files associated with this preprint. Click to download.

- [SupplMethods131020.pdf](#)